Design of Superresolved Phase Plates

Youhua Tan[1], Rui Guo[1], Shizhou Xiao[1], Guanghua Cheng[2], Wenhao Huang[1,*]

[1]*Department of Precision Machinery and Precision Instrumentation, University of Science and Technology of China, Hefei 230026*

[2]*State Key Laboratory of Transient Optics and Technology, Xi'an Institute of Optics and Precision Mechanics, Chinese Academy of Sciences, Xi'an 710068*

Abstract: Diffraction limit is always a key point to almost all optical systems, and diffraction effect is mostly dependent on the numerical aperture of objective and wavelength of light. However, it will be ultimately limited to improve the resolution continuously by increasing the numerical aperture or reducing the wavelength. Here, it is introduced that when these two parameters are fixed, focal spot smaller than Airy pattern could be obtained by means of superresolution techniques. Theoretical analysis for superresolution is presented. Binary phase plates corresponding to transverse or axial superresolution are designed, especially three-dimensional superresolution is proposed employing some optimization algorithms. The simulation results show that for light source with single wavelength or narrow spectral width, superresolution effects are fine, and when the superresolved phase plates are applied to femtosecond laser microfabrication system, the superresolution performances are even better when two-photon absorption is considered. Finally, the influences of spectrum of light sources are discussed. It has been demonstrated that when the spectral width is narrow, the performance of superresolved phase plates is approximately the same as that of a single wavelength. In conclusion, the superresoloved phase plates can be successfully applied to femtosecond laser systems for microfabrication, data memory and *et al*.

Keywords: superresolution, superresolved phase plate, laser microfabrication, optimization algorithm, compression ratio

1. Introduction

As it's well known that in a common optical system, the image of a point source is no longer a point but spreads over a certain spatial volume, and the optical distribution near focal spot has been well characterized as Airy pattern [1,2]. According to Rayleigh criterion, the focal spot size (d) is proportional to the wavelength (λ) of light source and inverse to the numerical aperture (NA) of the objective as: $d \propto \frac{\lambda}{NA}$, d can decrease by reducing λ or increasing NA. But in the practical applications, it will be ultimately limited to increase the numerical aperture or reduce the wavelength continuously. However, the exciting fact is that even when these parameters are fixed, the spot size can be further reduced by means of superresolution techniques [3].

The superresolution technique was a novel method to overcome the diffraction limit and improve resolution without the need to modify the optical apparatus significantly. It excited many researchers' interests: Sheppard [4-6] made much analytic study in the behavior of phase and amplitude plate filters, and they concluded that diffraction limit could be overcome in the transverse or axial direction; T. Sales [7,8] proved that when certain conditions such as Strehl ratio and sidelobe intensity were fixed, there existed fundamental limits of optical superresolution in both directions with phase-only superresolution elements; Daniel M. de Juana and Manuel P. Cagigal [9-12] designed a family of annular binary phase-only pupil filters and deduced the parameters of them analytically from the figures of merit that characterize the focal light intensity distribution,

furthermore, a superresolving continuous phase filters have been proposed. Due to its sub-diffraction superresolution, there are many applications including optical data storage, confocal scanning microscopy, imaging, and laser microfabrication. Recently, some of the applications have been reported: Changhe Zhou et al [13,14] designed a transverse-type phase filter and applied it in single-layer high density optical discs, and they achieved a transverse superresolution ratio of 0.8; Vidal F. Canales et al [12] reported a successful application of the superresolution technique in ground-based telescopes by use of rotationally symmetric pupil plate filters; Gilbert Boyer et al [15,16] inserted a three-ring amplitude filter in the illumination beam of two-photon scanning microscopy and derived a quasi-spherical shaped spot, which allowed the acquisition of three-dimensional images with isotropic quality.

As mentioned above, most of the literatures just solved the superresolution problems in either transverse or axial directions (refer to alternative directions) based on light sources with single wavelengths and few were applied to laser microfabrication systems. In this paper, three-dimensional superresolution is proposed and corresponding phase plate is designed with some optimization algorithms. Moreover, two types of phase plates are designed corresponding to superresolution in alternative directions respectively. As an application of these three types of phase plates in femtosecond laser microfabrication, the superresolution performances are even better when two-photon effect is considered. Finally, the spectral effects of light sources are discussed.

2. Theory of superresolution

It is useful to express the PSF (point spread function) of an aberration free optical system in normalized coordinates so that the diffraction limit can be always represented in a consistent manner, independent of details of numerical aperture or wavelength. In this way, the scalar field at the image plate U, assuming rotational symmetry and uniform illumination, is given by Fresnel approximation as following [1]:

$$U(\eta,\mu) = 2\int_0^1 T(r)J_0(\eta r)\exp(-i2\pi\mu r^2)rdr \quad (1)$$

where η is a normalized coordinate defined as $\eta = 2\pi NA\rho/\lambda$, with NA the numerical aperture of the system, λ the wavelength, and ρ the actual transverse coordinate at the image plane. μ is written as $\mu = (z-f)NA^2/2\lambda$, where $(z-f)$ measures the displacement from the focal point in actual units, and f denotes focal length of the focusing objective. The coordinate r at the exit pupil is normalized to one. The function $T(r)$ is a general complex pupil function $T(r) = A(r)\exp[i\varphi(r)]$, where $A(r)$ is the transmittance function and $\varphi(r)$ is the phase function. For simplicity, the intensity distribution provided by this pupil function can be expanded in series near the focal spot. The transverse and axial intensity distributions can be expressed to the second order as:

$$I_T(\eta,0) = |I_0|^2 - \frac{\eta^2}{2}\mathrm{Re}(I_0 I_1^*) \quad (2)$$

$$I_A(0,\mu) = |I_0|^2 - 4\pi\,\mathrm{Im}(I_0 I_1^*)\mu - 4\pi^2[\mathrm{Re}(I_0 I_2^*)$$
$$- |I_1|^2]\mu^2$$

$$(3)$$

where * denotes complex conjugate and I_m is the mth moment of the pupil function, defined as :

$$I_m = 2\int_0^1 T(r)r^{2m+1}dr \quad (4)$$

To characterize a given PSF we propose three basic vocabularies, which are all normalized by the counterparts of the Airy pattern (refers to the value $T(r)=1$). The spot size κ_T (κ_A) gives a measure of resolution and is defined as the first minimum of the superresolved pattern in transverse (axial) direction respectively. Occasionally we may also refer to the full-width at half-maximum (FWHM). The Strehl

ratio S denotes the central maximum intensity of PSF, by which reduction of the peak value can be well depicted. Finally the sidelobe intensity is measured by the quantity M, which includes the transverse sidelobe M_T and axial sidelobe M_A and determines the maximum value of the normalized intensity from the first minimum.

3. Design and simulation

To achieve superresolution and simplify the microfabrication process of superresolved plates, annular binary phase plates are considered.
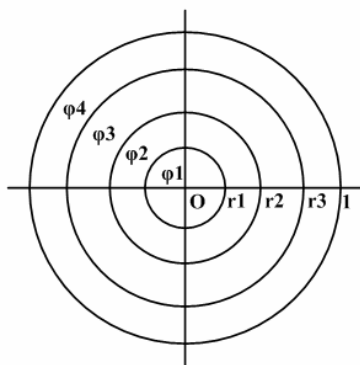
Fig1. The diagram of a phase plate

(the radius is normalized)

The plate consists of a number of zones (see Fig1), each of which is determined by its radius r and phase change φ. With equations (1)-(4), we can obtain the general expressions of the three basic quantities in these simple forms:

$$S = |I_0|^2 - 2\pi u_F \, \mathrm{Im}(I_0 I_1^*) \qquad (5)$$

$$\kappa_T = \sqrt{\frac{S}{2[\mathrm{Re}(I_0 I_1^*) - 4\pi u_F \, \mathrm{Im}(I_2 I_0^*)]}} \qquad (6)$$

$$\kappa_A = \sqrt{\frac{S}{12[\mathrm{Re}(I_0 I_2^*) - |I_0|^2]}} \qquad (7)$$

$$u_F = -\frac{1}{2\pi} \frac{\mathrm{Im}(I_0 I_1^*)}{\mathrm{Re}(I_0 I_2^*) - |I_1|^2} \qquad (8)$$

where u_F is the focus displacement and it's always zero for 0-π phase structure. Unfortunately, there is no analytical expression for the sidelobe intensity M.

As we know, traits of phase plates are

determined by zone numbers, radius and phase change of each zone, so appropriate design is very important. To obtain useful design for any given application, the design of phase plates must take into account simultaneous combination of spot size, Strehl ratio, and sidelobe intensity and it becomes necessary to determine optimal parameters satisfying a certain set of constrains. Here some optimization algorithms, such as genetic algorithm (GA) and global search algorithm (GSA) are employed. GA are algorithms that operate on a finite set of points, called a population [17]. The different populations are interpreted as generations. They are derived on the principles of natural selection and incorporate operators for (1) fitness assignment, (2) selection of points for recombination, (3) recombination of points, and (4) mutation of a point. The process of GA is shown as Fig.2. Crossover probability 0.85 and mutation probability 0.01 are applied, and global optimal solutions are obtained assisted by GSA [18]. GSA is an effective approach to solve continuous optimization problems subject to some constraints and its main process is as below: first, using the coordinate descent method to minimize the objective function with respect to each variable x_i, then we round off the variables, if it can reduce the number of selected attributes and satisfy the discernibility function, we save the round-off variables. And then we select next
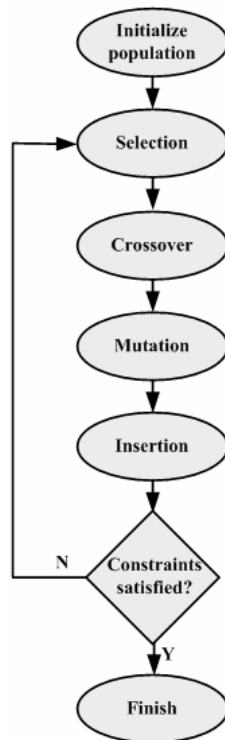
Fig2.Flow chart of GA

variable x_{i+1} for minimization. Generally, we must set the maximum search times and running time for termination of the algorithm.

With these algorithms, a whole family of four-zone binary phase plates is acquired, which realize transverse, axial, and three-dimensional superresolution respectively. The detailed design parameters and characterization quantities are shown in Table 1. The remarkable fact is that corresponding to superresolution in alternative directions, a simple 0-π phase structure is competent. However, to obtain superresolution in both directions simultaneously which is also called three-dimensional superresolution, multi-phase structure is needed. For the two kinds of design, when single-photon absorption takes place, the intensity distribution comparisons between superresolution pattern and Airy pattern are depicted by red and green line in Fig.3 respectively. First, the transverse spot size is reduced to 63% compared with Airy pattern (Fig3.a), and this is a high compression ratio. In contrast, we notice that the axial spot size is harder to compress and the intensity distribution in axial direction is more susceptible to the design parameters and difficult to control than that in transverse direction. However, by adjusting the crossover and mutation probability and a set of constraints very carefully in the process of optimization with GA and GSA, an acceptable axial compression ratio 0.80 is still obtained. Furthermore, even three-dimensional superresolution is realized. Fig3.c and d expresses the distinct superresolution effect in transverse and axial direction respectively. The simulation results demonstrate that the spot size is cut down to 89% in transverse direction and 69% in the other and focus displacement is controlled to very small. Besides, the quantities M_T and M_A are used to evaluate the superresolution effect of phase plates, and we notice that the axial sidelobe intensity M_A is generally stronger than M_T and when the design parameters vary slightly, M_A may make a leap. Nevertheless, the above results clearly imply that using these kinds of phase elements central diffraction spots can be successfully compressed.

Table1 optimized design parameter

Superresolution	S	κ_T	κ_A	M_T	M_A	u_F	r_1	r_2	r_3	φ_1	φ_2	φ_3	φ_4
Transverse	0.20	0.63	—	0.08	—	0	0.153	0.253	0.563	0	π	0	π
Axial	0.37	—	0.80	—	0.22	0	0.200	0.730	0.830	0	π	0	π
3D	0.35	0.89	0.69	0.03	0.20	-0.0003	0.337	0.478	0.658	3.032	3.132	0	2.989
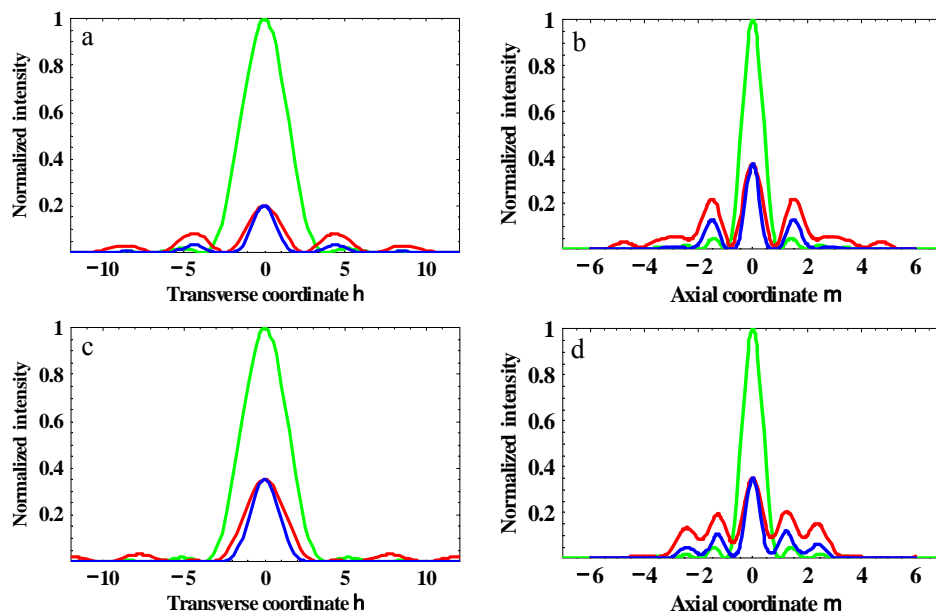
Fig3. Theoretical comparisons of superresolution pattern and Airy pattern: superresolution only in (a)transverse, (b) axial, (c) and (d) transverse and axial direction simultaneously, where green line denotes Airy pattern, red line denotes single-photon absorption superresolution pattern and blue line denotes two-photon absorption superresolution pattern

4. Discussions

As proved in section 3, although a phase plate can reduce the focal spot size, it actually creates strong sidelobes simultaneously, as can be seen in Fig.3. However, when it is applied to laser microfabrication, this side-effect can be suppressed by multi-photon absorption, especially two-photon absorption in our femtosecond laser fabrication system [19,20], which is highly nonlinear and dependent on the peak intensity. As expressed in Fig.3, the blue line denotes two-photon absorption superresolution pattern and it can be clearly seen that when two-photon nonlinear absorption happens, the superresolved phase plates have better resolution and lower sidelobes, and this is one of the advantages of femtosecond laser fabrication.

Another issue for its application in laser fabrication is that all mentioned above are based on single wavelength light sources while femtosecond laser pulse actually has a certain spectral width. As we know, the phase change φ_i of each zone of phase plates is as follows:

$$\varphi_i = \frac{2\pi}{\lambda}(n-1)d_i \qquad (9)$$

where d_i is the depth of each zone and n is the refraction index of a phase plate. Therefore, if the optimization design focuses on a single wavelength λ_0, φ_i and r_i are determined and relevant d_i are also fixed, then all parameters of a phase plate are decided. When another light source with wavelength λ is used, φ_i alter and pupil function $T(r)$ changes, so the superresolution performance varies. Fig. 4 describes the influences of multiple wavelengths on the performance of superresolved phase plates. For simplicity, three light wavelengths with uniform proportion of intensity are

considered and the calculation method is similar to that of single wavelength case. The phase plates are designed based on single wavelength λ_0=800nm which is represented by red line. Blue line denotes the superresolved pattern when λ_0=800nm, λ_1=780nm and λ_2=820nm, and this is the situation of our femtosecond laser system whose wavelength centers in 800nm, and spectrum range is from 780nm to 820nm. In Fig.4, it shows that when three kinds of light wavelengths (780nm, 800nm and 820nm) are introduced, the superresolution performance is approximately the same as that of a single wavelength (800nm) and therefore, the blue lines and red lines are overlapping. However, if the spectral width becomes broad, for instance, λ_0=800nm, λ_1=600nm, λ_2=1000nm, the situation becomes rather bad which is represented by green lines. A feasible solution to this issue is that design of phase plates is based on the whole spectral range, but the problem will become more complex. In conclusion, for usual femtosecond laser fabrication systems with narrow spectral width, the performance of superresolved phase plates is so good that they will have potential applications in this area.

5. Conclusions

In summary, three-dimensional superresolution is proposed and the optimized design of a family of superresolved annular phase plates has been presented. When this type of superresolved phase plates applied in femtosecond laser fabrication system, the performance is even better while nonlinear absorption effect is considered. Finally, the influences of spectrum of light sources are discussed.

Acknowledgements
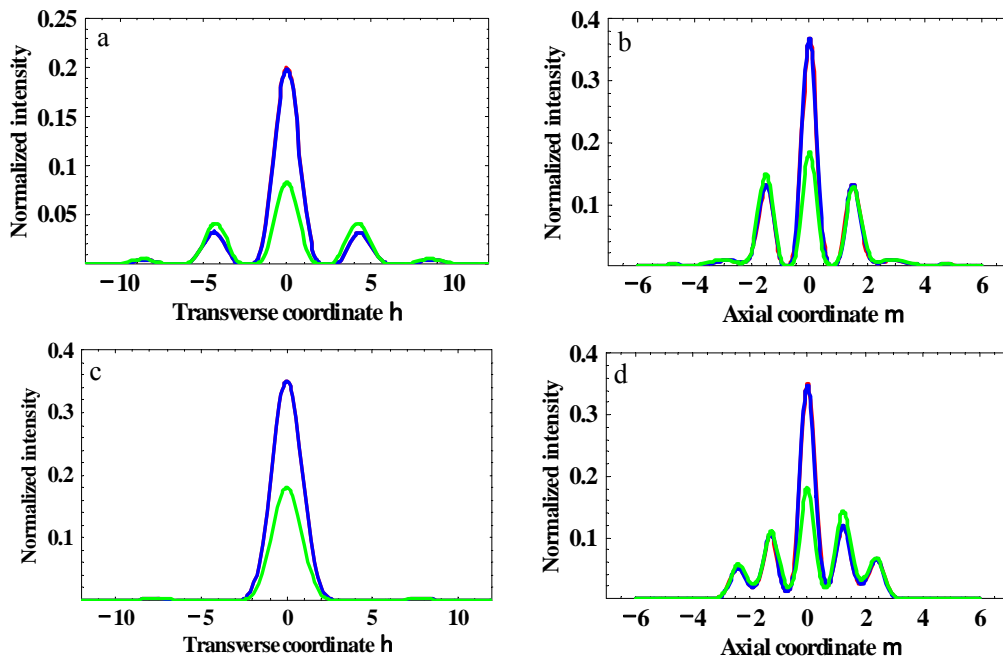
Fig4. Comparison of two-photon absorption superresolution patterns when multiple wavelengths are considered: superresolution only in (a)transverse, (b) axial, (c) and (d) both direction(s) simultaneously, where red line denotes single wavelength light source λ_0=800nm, blue line denotes the situation which includes three kinds of wavelengths λ_0=800nm, λ_1=780nm, λ_2=820nm and wavelengths of green line are λ_0=800nm, λ_1=600nm, λ_2=1000nm. Note that the blue lines and red lines are approximately overlapping and the proportions of each spectral component are uniform.

References:

1. M.Born and E. Wolf, *Principles of Optics* (Pergamon, New York, 1975)

2. Satoshi Kawata, Hong-Bo Sun, Tomokazu Tanaka, Kenji Takada, *Nature*, 412, 697 (2001)

3. G. Toraldo di Francia, *Nuovo Cimento Suppl.* 9, 426 (1952)

4. C.J.R.Sheppard, and Z.S.Hegedus, *J.Opt.Soc.Am A*, 5, 643 (1988)

5. C.J.R.Sheppard, G.Calvert, and M. Wheatland, *J.Opt.Soc.Am.A*, 15, 849 (1998)

6. C.J.R.Sheppard, and A.Choudhury, *App. Opt.* 43,4322 (2004)

7. Tasso R.M. Sales, and G. M. Morris, *Optics Letters*, 22, 582 (1997)

8. Tasso R.M. Sales, *Phys. Rev. Lett.* 81,3844 (1998)

9. Daniel M. de Juana, Jose E. Oti, Vidal F. Canales, and Manuel P. Cagigal, *Optics letters*, 28, 607 (2003)

10. Daniel M. de Juana, Vidal F. Canales, Pedro J. Valle, and Manuel P. Cagigal, *Optics Communication,* 229, 71 (2004)

11. Manuel P. Cagigal, Jose E. Oti, Vidal F. Canales, and Pedro J. Valle, *Optics Communication,* 241, 249 (2004)

12. Vidal F. Canales, Daniel M. de Juana, and Manuel P. Cagigal, *Optics Letters*, 29, 935 (2004)

13. S. Zhou, Changhe Zhou, *Optics Letters*, 29, 2746 (2004)

14. Changhe Zhou, Hongxin Luo, *SPIE,* 5966, 596615-1 (2005)

15. Cristina Ibanez-lopez, Genaro Saavedra, Karsten Plamann, Gilbert Boyer, and Manuel Martinez-Corral, *Microscopy research and technique*, 67,22 (2005)

16. Cristina Ibanez-lopez, Genaro Saavedra, and Gilbert Boyer, *Optics Express*, 13, 6168 (2005)

17. Goldberg D.E., *Genetic algorithms in*

search, optimisation, and machine learning. (Addison-Wesley; 1989)

18. J. Gu, *IEEE Trans. On Knowledge and Data Engineering,* 6, 361 (1994)

19. R. Guo, Z. Y. Li,Z. W. Jiang, D. J. Yuan, W. H. Huang and A. D. Xia, *J. Opt. A: Pure Appl. Opt.* **7**, 396 (2005)

20. R. Guo, S. Z. Xiao, X. M. Zhai, J. W. Li, A. D. Xia and W. H. Huang, *Opt. Express*, 14, 810 (2006)